Hindawi
Journal of Chemistry
Volume 2020, Article ID 6667450, 11 pages
https://doi.org/10.1155/2020/6667450

Research Article

Antifungal Activity of Gelatin-Tapioca Starch Film and Coating Containing Copper Nanoparticles against *Colletotrichum gloeosporioides* Causing Anthracnose

Vinh Tien Nguyen, My-Sam Dang-Thi, and Khanh Son Trinh

Ho Chi Minh City University of Technology and Education, 1 Vo Van Ngan Street, Thu Duc District, Ho Chi Minh City, Vietnam

Correspondence should be addressed to Khanh Son Trinh; sontk@hcmute.edu.vn

Received 7 October 2020; Revised 25 November 2020; Accepted 14 December 2020; Published 28 December 2020

Academic Editor: Francisco Javier Deive

This study aimed to fabricate a nontoxic coating containing copper nanoparticles (CuNPs) to protect fruits from pathogenic *Colletotrichum gloeosporioides* causing anthracnose on several tropical fruits. We used a green approach, in which CuNPs were synthesized by reducing $CuSO_4$ with ascorbic acid in the presence of gelatin and glycerol as the capping agents. The formation of CuNPs was confirmed by UV-vis absorption spectra of the reaction mixture, which showed a surface plasmon resonance peak at 578–594 nm. The x-ray diffraction spectrum of the CuNPs indicated the presence of mostly metallic copper with some minor impurities of Cu_2O, CuO, and $Cu(OH)_2$. Transmission electron microscopy (TEM) images and dynamic light scattering studies showed that the sizes of 90% of CuNPs were in 100–300 nm range. A 30–50 nm capping layer of gelatin surrounding CuNPs can be observed in the TEM images. Comparing FTIR spectra of the used reagents and CuNPs confirmed the depletion of ascorbic acid, as well as the gelatin layer protecting CuNPs. The synthesized CuNPs showed dose-dependent antifungal activity against *C. gloeosporioides* with 100% growth inhibition at 200 ppm copper. Gelatinized tapioca starch was then added to the CuNPs solution to obtain a film-forming mixture to produce stand-alone composite films on Petri dishes and coatings on mangoes. *C. gloeosporioides* could not grow on the surface of nutrient agar in contact with the films containing 245 ppm CuNPs, while they grew normally on control films without CuNPs. For the *in vivo* antifungal tests on mangoes, both the control and the CuNPs-containing coatings equally inhibit fungal growth, possibly due to the low oxygen permeability of the protein and starch components in the films. This study thus demonstrated the potential applications of composite coatings using biodegradable polymers that contain CuNPs in postharvest protecting fruits from phytopathogenic fungi.

1. Introduction

Mango (*Mangifera indica* L.) is one of the most popular tropical fruits due to its strong and attractive aroma, delicious taste, high nutritional value, and bright yellow colours of peel and flesh [1]. However, anthracnose caused by *Colletotrichum gloeosporioides* is one of the most severe diseases causing postharvest losses in mango during storage and transportation. Anthracnose can cause 30–60% damage, and sometimes up to 100% for mangoes produced under wet or humid conditions. Besides mango, anthracnose also contributes significantly to preharvest and postharvest losses of other crops, such as cashew, papaya, pomegranate, guava, and acid lime [2].

Many methods have been developed to fight anthracnose in fruits, but each of them has its strengths and weaknesses. Chemical control by direct spraying fungicides on fruits is highly effective but may result in resistance of the pathogens and high levels of residue [3]. Many natural essential oils are emerging as effective and safe biofungicides, but they are volatile, and their high contents may affect the intrinsic aroma and taste of the protected fruits [4]. Heat treatment by dipping fruits in hot water is a simple, nontoxic, and moderately effective method but can easily cause overheat damage to the fruits [5]. Gamma irradiation or biological antagonists have high cost and low effectiveness and require specific legislation [6,7]. Until now, a sequential or simultaneous combination of hot water and fungicide is the most

effective commercial postharvest treatment for mango anthracnose.

Among the emerging techniques to fight anthracnoses in fruits, surface coatings incorporated with antimicrobial agents are a promising solution with several additional advantages: a glossy appearance of the fruit surface, reduced weight loss of fruit, delayed ripening, controlled release of active components, and extended storage life [8]. The fruit coatings can be natural polymers, such as chitosan, starch, gelatin, agar, alginate, or synthetic polymers, such as polyethylene, carboxymethyl cellulose, and copolymers [9]. The polymeric matrix of fruit coatings should desirably be nontoxic, biodegradable, transparent, and tunable in barrier properties against water vapour, CO_2, oxygen, and ethylene.

It should be noted that although films and coatings are usually used as synonyms, they refer to different concepts according to their purpose and utilization. A film is a stand-alone thin layer of material that can be used as cover, wrap, or separation layer. On the other hand, coatings are films formed directly on the surface of the product that they are intended to be utilized with. Speaking another way, the coating is a part of the final product.

For antimicrobial coatings, antimicrobial agents are added to the packaging materials to avoid direct contact and control the release of the preservatives. Many antimicrobial agents were successfully incorporated into food coatings and exhibited strong inhibition of bacterial and fungal growth: commercial preservatives [10,11], fungicides [12], plant extracts [13], essential oils [14], and nanoparticles [15,16].

Metal nanoparticles possess unique properties like physicochemical, electrical, optical, and biological, which are much different from their bulk metals. Extensive studies have proved the antimicrobial activity of metal nanoparticles. This property is due to their small size and high surface-to-volume ratio, which enhance their interactions with a broad spectrum of microorganisms. Silver nanoparticles are the most investigated nanoparticles with high biocidal effects on bacteria, fungi, and viruses [17]. However, the high price of silver significantly hinders its application range. The low price and the high antimicrobial activity of copper nanoparticles (CuNPs) make them an attractive alternative to silver nanoparticles in antimicrobial packaging for the food industry [18]. Metallic copper and copper compounds have a long history of being used as antibacterial and antifungal agents in agriculture and medicine [19,20]. CuNPs synthesized by *Ocimum sanctum* leaf extract showed growth inhibition activity against 11 fungal phytopathogens, including *C. gloeosporioides* [21]. During its antifungal actions, CuNPs change the colour, morphology, form, texture, and density of the fungal mycelia [22]. Among the approaches for CuNPs synthesis, chemical reduction is the most common and convenient. In this approach, copper (I or II) salts are reduced by medium-to-strong reducing agents, such as $NaBH_4$, hydrazine, and hypophosphite, which are usually toxic [23]. Moreover, to produce CuNPs, the reduction of copper ions must be carried out in the presence of capping molecules, which adsorb onto surface of the formed CuNPs and prevent them from growing further in size.

To be applied for fruit coatings, nontoxic substances must be used in the fabrication of CuNPs and active coatings. Therefore, in this study, we used a green method of CuNPs synthesis: reducing $CuSO_4$ with ascorbic acid (AA) in the presence of gelatin and glycerol as dual capping agents and stabilizers for CuNPs. The one-pot technique was used to fabricate CuNPs-containing films and coatings: freshly synthesized CuNPs solution was combined with gelatinized tapioca starch to obtain a film-forming mixture. To evaluate the antifungal activity against *C. gloeosporioides,* CuNPs and the stand-alone films containing CuNPs were tested *in vitro* on Petri dishes, while the coatings were tested *in vivo* on mangoes.

2. Materials and Methods

2.1. Chemicals and Materials. Gelatin, glycerol, copper sulfate, and ascorbic acid were purchased from Xilong Scientific LTD (China) with analytical grades. Tapioca starch and mangoes were purchased from a local supermarket in Ho Chi Minh City, Vietnam. The nutrient broth and agar were purchased from Himedia (India).

2.2. Preparation of CuNPs Solution. CuNPs were synthesized based on a published method with some modifications [24]. An aqueous solution of 0.01 M $CuSO_4$ (50 mL) containing 4 g of gelatin and 3 g of glycerol was prepared and magnetically stirred for the complete dissolution of gelatin. After that, the solution was heated to 80°C and 50 mL of 0.05 M AA was added. The reaction mixture was kept at 80°C with continuous stirring for 90 min and then cooled to room temperature.

2.3. Formation of Composite Films Containing CuNPs. Tapioca starch was dispersed in distilled water (5%, *w/v*) and gelatinized at 95°C for 30 min. The gel was cooled to 50°C and the CuNPs solution was added to obtain a mixture with 245 ppm of copper. The mixture was stirred for 1 h while cooling to room temperature. Every 7.0 mL of the film-forming mixture was poured onto a Petri dish (diameter 9.0 cm) and dried at 45°C for 48 h in a convection oven. The dried films were peeled off and conditioned in a chamber with a constant relative humidity of 80% (using a saturated solution of NaCl) at least 48 h before further experiments.

A control film was prepared with the same procedure, but the added CuNPs solution was replaced by the same volume of distilled water.

2.3.1. CuNPs Characterization. Absorption UV-vis spectra of the CuNPs solution were recorded from 400 to 800 nm using a UH5300 spectrophotometer (Hitachi, Japan).

To obtain solid CuNPs for FTIR characterization, the CuNPs solution was vacuum-dried at 60°C for 6 h and the obtained solid was finely ground and mixed with KBr to a final KBr/solid ratio of 200. ATR-FTIR spectrum of the mixture was recorded from 4000 to 400 cm^{-1} with a resolution of 2 cm^{-1} on a Jasco FT/IR 4700 spectrometer (Germany).

For XRD characterization, CuNPs were centrifuged at 10,000 rpm for 30 min and washed twice with deionized water. XRD spectrum of CuNPs was recorded on a D8-Advance x-ray diffractometer (Bruker, Germany) with 2θ from 20° to 90°. The operation parameters were 40 kV potential, 40 mA current, and Cu-Kα wavelength of 1.5406 Å.

The size distribution of CuNPs in the solution was recorded using the dynamic light scattering (DLS) method on a HORIBA LA-920 (Japan).

Transmission electron microscopy (TEM) was used on a JEM-1400 (JEOL, Japan) to record the size and shape of CuNPs in solution at a voltage of 100 kV.

Scanning electron microscope JEOL 5410 LV (Japan) was used to observe the cross-sections and surfaces of the films on Petri dishes and the coatings on mango.

2.3.2. In Vitro Antifungal Activity of CuNPs Solution. *In vitro* antifungal activity of CuNPs against *C. gloeosporioides* was evaluated based on a published method [22]. The CuNPs solution was mixed with 25 mL of melted nutrient broth (NB) agar medium to reach predetermined copper concentrations of 0, 50, 100, 150, and 200 ppm. The mixtures were poured onto Petri dishes and left cooling to room temperature. Mycelia of *C. gloeosporioides* were then put onto the centre of each Petri dish. The dishes infected with *C. gloeosporioides* were incubated at 30°C for 10 days.

The antifungal tests were also conducted for 3 control dishes containing each of the following instead of CuNPs: (i) 500 ppm $CuSO_4$; (ii) 2200 ppm AA; and (iii) 20% mango flesh (to confirm the growability of the fungus on mango).

The size of each fungal colony was evaluated as the average of two perpendicular diameters. The percent inhibition of radial growth (IRG) of *C. gloeosporioides* was calculated as follows:

$$\text{IRG}(\%) = \frac{d_0 - d_1}{d_0} \times 100, \quad (1)$$

where d_0 and d_1 are the average diameters of the colonies in the dish containing no copper and that containing CuNPs, respectively. All dishes were triplicated.

2.3.3. In Vitro Antifungal Activity of Composite Films Containing CuNPs. One-week-old fungal mycelia of *C. gloeosporioides* were dispersed in 1.0 mL of sterile distilled water and then spread onto the surface of NB agar dishes. Films containing 245 ppm CuNPs were cut 3 × 3 cm and put on the agar surface infected with the fungus. The blank was an infected agar dish without films and the control was a dish with the tapioca starch-gelatin film not containing CuNPs. The radial mycelial growth of *C. gloeosporioides* colonies on these Petri dishes was measured for 48 h. All Petri dishes were triplicated.

2.3.4. In Vivo Antifungal Activity of Coatings on Mango. The *in vivo* antifungal tests were adapted from a published method with some modifications [25]. Mangoes (*Moringa oleifera*) at moderate ripeness (4 fruits/kg) were washed successively with tap water and then with 70% ethanol to disinfect the fruit surface. The sterile fruit surface was pricked with a sterile needle to form 9 small holes of 3 mm depth. Each hole was subsequently injected with 20 μL of *C. gloeosporioides* mycelia in sterile water and left 2 h for drying. The first 50 mL portion of the film-forming solution was poured and spread carefully on the fruit surface to ensure a uniform coating. After 1 h of partial drying at room temperature, a second 50 mL portion of the film-forming solution was poured on the first layer. The sizes of developing fungal colonies on the fruit surface were measured for 4 days and IRG was calculated according to formula (1). All coated and uncoated mangoes were triplicated.

3. Results and Discussion

3.1. Formation and Characterization of CuNPs. Copper(II) ions are reduced by several agents, such as NaBH4, hydrazine, and AA. Because the work orients on applications in food packaging, we chose AA based on its safety to human health and the environment. In the reaction with AA in solution, copper(II) ions are first converted to $Cu(OH)_2$, which is then reduced successively to Cu_2O and Cu, or CuNPs [26]. In our reaction system, gelatin and glycerol played the role of dual capping agents that protect CuNPs from growing in size. At the same time, gelatin also served as one of the polymeric materials in the composite film, and glycerol as the plasticizer for the film [27].

The dark brown-red colour of the reaction mixture after 90 min (inset of Figure 1) demonstrates the formation of metallic copper [24]. Moreover, UV-vis spectra of the reaction mixture at 30–120 min of reaction (Figure 1) show a peak at 578–594 nm, which is characteristic for surface plasmon resonance of CuNPs [24,28]. The unchanged height of this peak after 60 min implied that the formation of CuNPs almost finished after that time. However, the spectral part with wavelengths below 570 nm still rose after 60 min, demonstrating that some side reaction(s) still occurred. We suggest that the excess AA was being oxidized by oxygen in the air.

The size distribution of CuNPs in the reaction mixture after 90 min (Figure 2) shows that their size ranged from 90 to 510 nm, in which 90% of CuNPs were smaller than 300 nm and 50% of them smaller than 200 nm. These sizes were higher than those in other studies due to the low molar ratio of AA : $CuSO_4$ (5 : 1) [28,29]. However, for an application-oriented study like this, a high excess of AA is cost-ineffective. Moreover, too small CuNPs are not stable against oxidation by air oxygen [30].

TEM images of CuNPs in the reaction mixture (Figure 3) show that most of the CuNPs are smaller than 300 nm, which agrees with the DLS size distribution. A 20–50 nm thin layer of gelatin-glycerol capping agents surrounds each particle (red arrows). This polymeric layer was formed due to the intermolecular interactions between functional groups of gelatin and glycerol with the surface of CuNPs [31]. We suggest that these intermolecular interactions are electrostatic attractions between negatively charged electron clouds on the surface of metallic CuNPs with positively charged

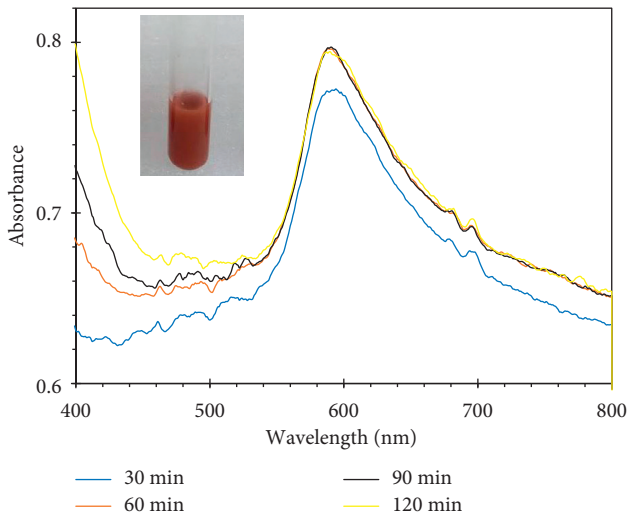

Figure 1: UV-vis spectra of the reaction mixture over time. Inset: the appearance of the reaction mixture at 90 min.

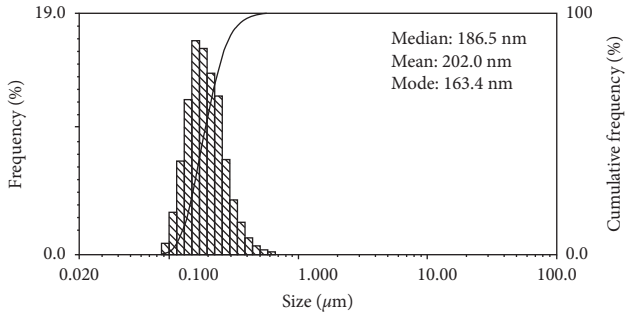

Figure 2: DLS size distribution of CuNPs in solution after 90 min of reaction.

hydrogen atoms in –OH groups in glycerol and protonated $-NH_2$ groups in gelatin molecules. The capping layer serves as a cushion that prevents the adhesion of CuNPs upon their collisions. TEM images of CuNPs in other studies using polyvinyl pyrrolidone as the capping agent also showed similar thin protecting layers of about 5–8 nm [32,33].

TEM images also show the aggregation of CuNPs into bigger particles. The light areas in many aggregates or particles (yellow arrows) indicate the places where the particles did not "fit" each other upon aggregation, thus forming "holes" in the aggregates. These holes increase the surface areas of the aggregates and therefore can facilitate the release of antimicrobial copper ions into the medium.

XRD spectrum of the synthesized CuNPs product (Figure 4) shows sharp and high characteristic peaks at 2θ of 43.31°, 50.40°, and 74.17°, which correspond to (111), (200), and (220) planes in standard JCPDS-04-0836 for metallic copper crystals [26]. These peaks confirmed the formation of mainly copper metal in the reaction between $CuSO_4$ and AA. Some small peaks of Cu_2O, CuO, and $Cu(OH)_2$ impurities in the XRD spectrum [34] were possibly due to surface oxidation of metallic copper by oxygen in the air or incomplete reduction of copper(II) by AA [30,35].

Figure 5 shows the ATR-FTIR spectra of glycerol (a), AA (b), gelatin (c), and the CuNPs-containing powder obtained after vacuum-drying the reactive solution (d).

In the spectrum of glycerol, the strong and broad peak at 3200–3540 cm^{-1} corresponds to O-H stretching and the double peak at 2950 corresponds to C-H stretching. These two characteristics peaks of glycerol also appeared on the spectrum of CuNPs powder, hence indicating that glycerol remained in the CuNPs powder and may be involved in the capping layer of CuNPs [36].

In the spectrum of AA, four characteristic peaks at 3523, 3406, 3307, and 3228 cm^{-1} correspond to four O-H groups in the molecule. These four peaks disappeared on the CuNPs powder spectrum indicating complete oxidation of AA by copper ions and air oxygen [37]. The 1670 cm^{-1} peak corresponding to the C-O-C group and the 1757 cm^{-1} peak corresponding to the lactone C=O stretching in AA also appeared in the CuNPs spectrum [38]. However, looking at the relative intensities of these two peaks in the CuNPs powder spectrum, one can recognize that the height of the 1652 cm^{-1} peak in CuNPs spectrum has increased significantly. This is due to the presence of the 1659 cm^{-1} amide I band of the gelatin present as a capping agent for CuNPs [37].

3.2. SEM Images of Cross-Sections of the Composite Films. Figure 6 shows the cross-sections of the composite film cast on a Petri dish (a1–e1) and the composite coating on a mango surface (a_2–f_2). The average thickness (from 12 positions) of the coating was about 16 ± 1 μm, which was much lower than that of the film of 48 ± 2 μm (Figure 4, d_2-e_2). This was because the low adhesive force between the film-forming solution and the mango surface kept only a thin layer of the former on the latter.

The film and the coating surfaces in Figure 6 a_1 and a_2 had uniform morphology and without cracks or holes, possibly because of the flexibility of gelatin and the plasticizing effect of glycerol [39]. However, holes and channels can be observed in the cross-sections of the coating (Figure 6 a2, b2), possibly due to the continuous transmission of water vapour from the fruit to the air.

Particles of 2–5 μm can be observed in the cross-section of the films (red arrows in Figures 6 b_1, e_1, d_2). These sizes are about 10–30 times bigger than those obtained in TEM and DLS analysis of CuNPs sizes. This result indicates that, during the starch gelatinization and the film formation, CuNPs can aggregate into larger clusters. As discussed in the following section, the antimicrobial activity of the composite films is based on the release of copper ions to the medium. Therefore, the aggregation of CuNPs in the film matrix is undesirable, because it reduces the surface area and the releasing ability of CuNP, which in turn reduces the antimicrobial effect of the film. However, larger sizes of CuNP make the release of copper ions more sustained over a longer time and prevent the risk of a high concentration of released copper, which may diffuse into the peel and flesh of the coated fruit. For applications that require smaller CuNPs and more homogeneous films, we suggest adding more

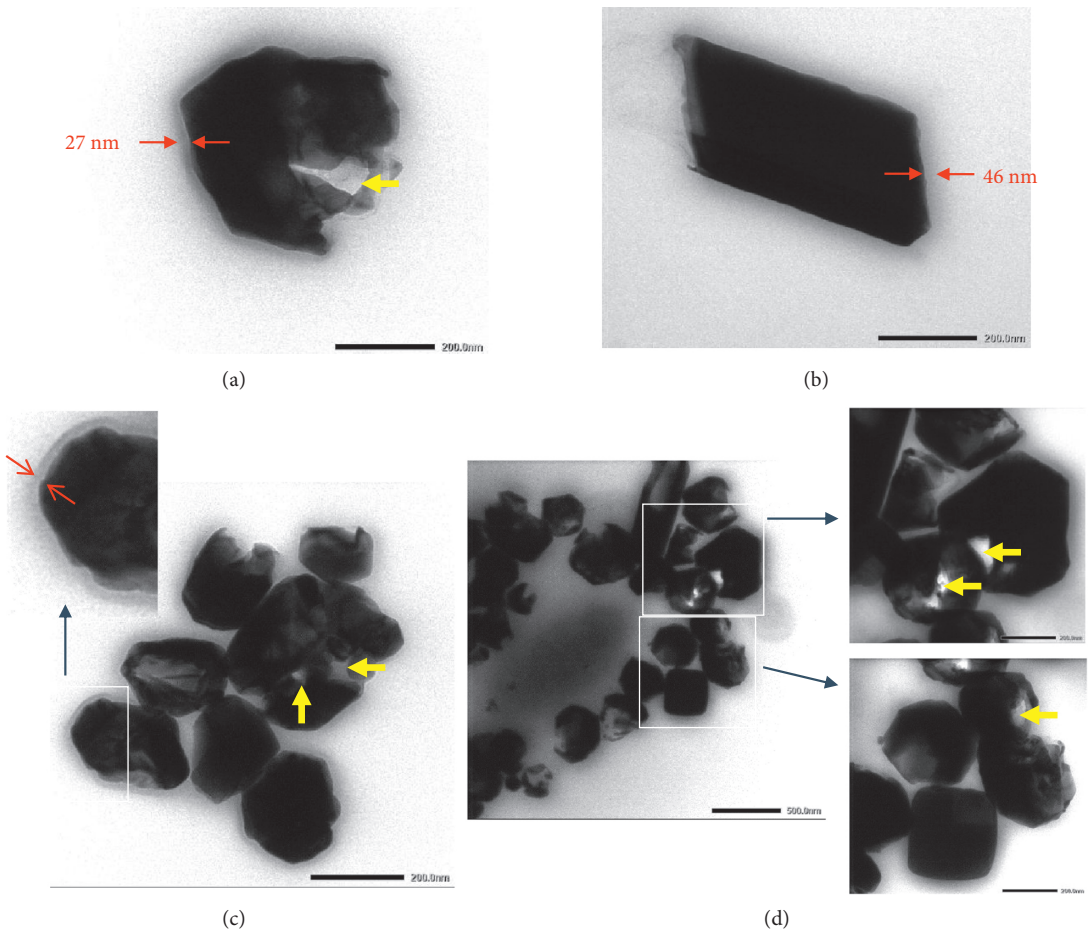

Figure 3: TEM images of CuNPs in solution after 90 min of reaction. Blue arrows point to magnified areas in the white rectangles. Red arrows show the capping layers surrounding CuNPs. Yellow arrows show "holes" inside CuNP aggregates.

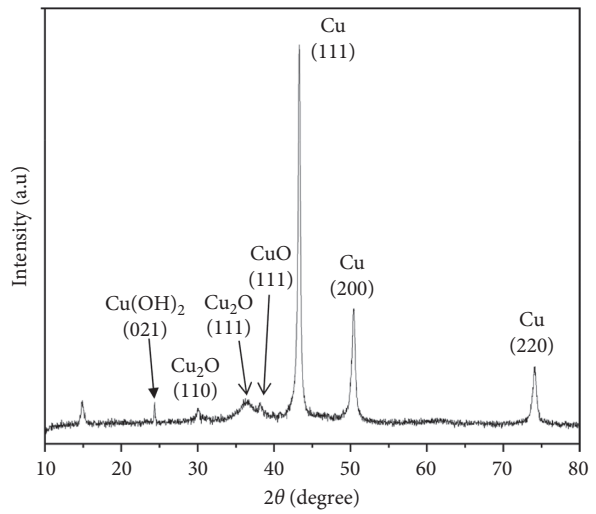

Figure 4: XRD spectrum of CuNPs centrifuged after 90 min of reaction.

polymer components (gelatin and/or starch) before the film-forming step to make the solution more viscous and prevent CuNP aggregation during the film drying.

3.3. In Vitro Antifungal Test of CuNPs against C. gloeosporioides. The 500 ppm CuNPs solution was mixed with the NB medium to final copper concentrations of 100,

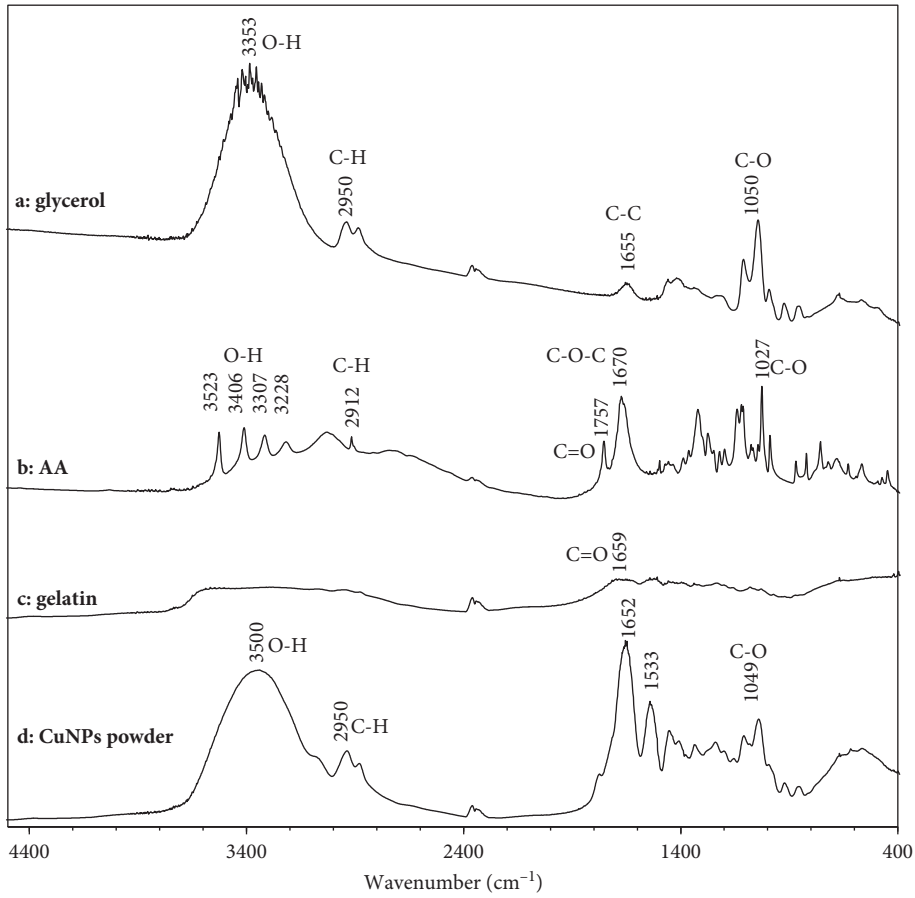

Figure 5: ATR-FTIR spectra of glycerol, AA, gelatin, and CuNPs-containing powder.

150, and 200 ppm. These CuNPs-containing nutrient media, together with other control nutrient media containing 20% mango flesh, 2200 ppm AA, or 500 ppm $CuSO_4$, were used to incubate *C. gloeosporioides* on Petri dishes. A strong inhibition effect results in smaller colony size, compared to that in the blank control. Figure 7 shows that mango flesh (7b) and AA (7c) exhibit some antifungal activity because their acidity can inhibit the respiration of the fungi [40]. Copper ions from 500 ppm $CuSO_4$ 100% inhibited the growth of *C. gloeosporioides* (7d), which is their well-known property [20]. Figures 7(e)–7(g) show concentration-dependent antifungal activity of CuNPs with 100% inhibition at 200 ppm of CuNPs.

Figure 8 shows the growth dynamics of the *C. gloeosporioides* colonies on Petri dishes. In the first 3 days, the fungus grew on the mango flesh control faster than on the blank, possibly due to the nutrient ingredients in the mango. The concentration-dependent antifungal activity of CuNPs can be observed on the whole time range of the experiment. Due to the immobility of solid particles in the solid agar medium, the antifungal activity of CuNPs is attributable to the release of copper ions from CuNPs to the medium [41]. The antifungal activity of the $CuSO_4$ control can confirm this hypothesis. Moreover, many studies have shown the ease of oxidation of CuNPs to copper ions in the presence of air [22,41]. The cytotoxicity mechanisms of copper ions are well studied: they induce the formation of hydroxyl radicals when getting in contact with the cell membrane; these radicals result in the oxidative degradation of the lipids composing the cell membrane, the subsequent leakage of intracellular substances, such as K^+ ions [42], the alteration of intracellular biochemical processes, and finally cell death [43].

It is known that $CuSO_4$ begins exhibiting antifungal activity at 5–100 ppm; and in our experiments, $CuSO_4$ at 500 ppm inhibited 100% the growth of *C. gloeosporioides* [44]. However, it should be noted that using $CuSO_4$ in fruit coatings is undesirable due to the possible diffusion of abundant copper ions from the coating to the fruit peel. In contrast, bigger CuNPs are immobilized in the polymer matrix, and the oxidative release of copper ions from the surface of CuNPs is gradual, thus lowering the risk of copper contamination in the fruit peel. In this study, 100% inhibition of *C. gloeosporioides* growth at 200 ppm or 0.2 mg/mL of copper is high antifungal activity. For the sake of comparison, CuNPs synthesized using AA showed 100% growth inhibition against *Fusarium solani*, *Neofusicoccum* sp., and *Fusarium oxysporum* only at concentrations higher than 0.75 mg/mL.

3.4. In Vitro Antifungal Activity of Tapioca Starch/Gelatin Films Containing CuNPs. Figure 9 shows that *C. gloeosporioides* grew on the control dish more strongly,

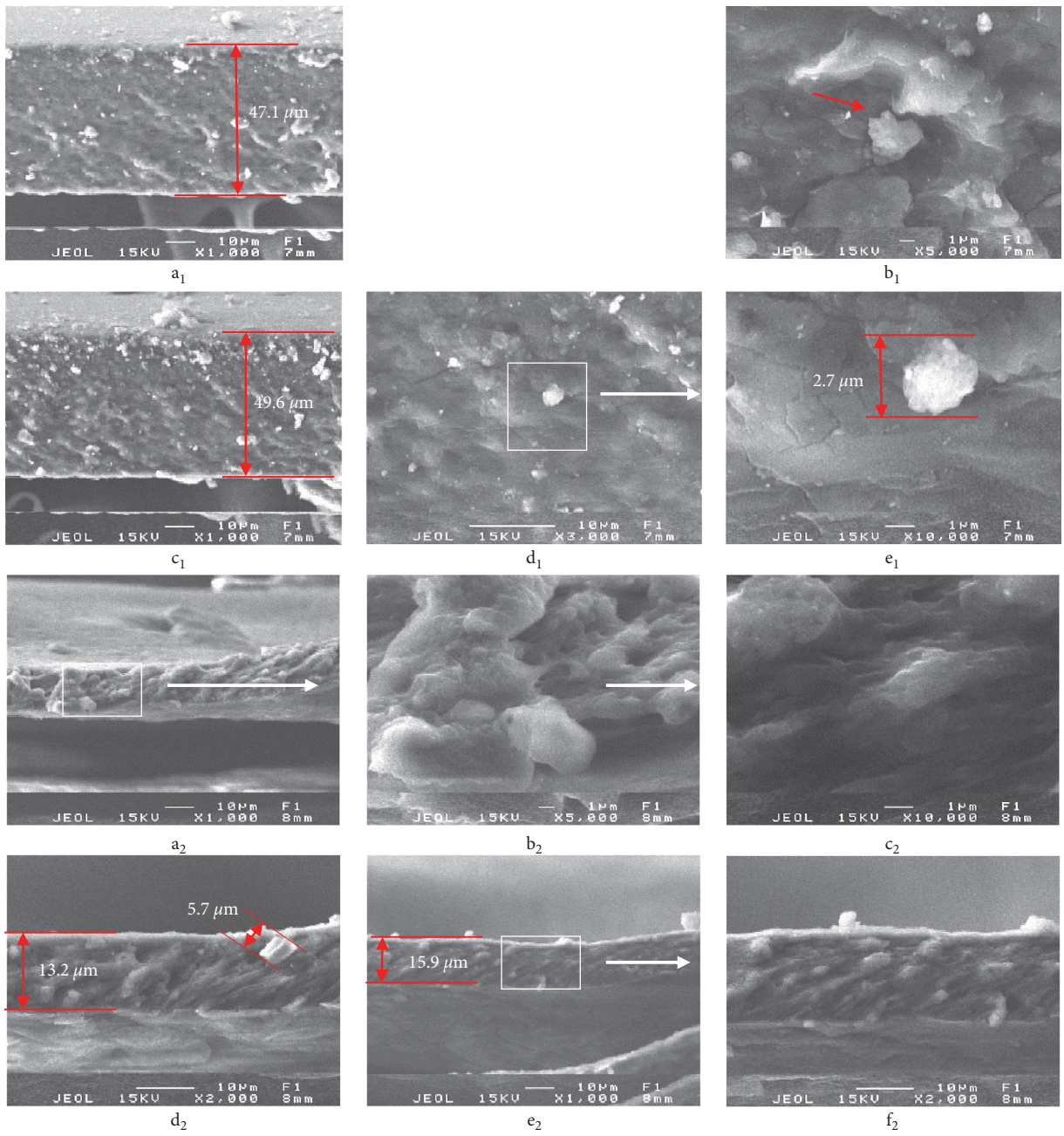

FIGURE 6: SEM images of cross-sections of the composite films containing CuNPs: (a_1–e_1) on Petri dishes, (a_2–f_2) on the surface of mangoes. White rectangles and arrows indicate magnified areas on the next figure.

compared to the blank dish. The fungus grew under, and even on, the control film because gelatin and starch are nutritional components favouring the fungal growth. In contrast, *C. gloeosporioides* could not grow on, and even under, the composite film containing 245 ppm CuNPs. This result indicates that CuNPs imparted the antifungal property not only to the composite film, but also to the agar surface. The agar surface acquired antifungal properties possibly because of the diffusion of antifungal copper ions from the film to the agar.

3.5. In Vivo Antifungal Activity of CuNPs-Containing Films on Mango Surface. The coatings on mango in our study were very thin (30–50 μm from Figure 6 a_2–d_2), hence keeping the colour of the fruit peel not affected by the red-brown CuNPs. Moreover, the tapioca starch-gelatin imparts a glossy appearance to the fruit (Figures 10 a, c, and d compared to b).

Figure 10(b) shows that, after 4 days of infection, the *C. gloeosporioides* significantly developed on the surface of uncoated mangoes. At the same time, the mangoes coated with control film (Figure 10(c)) and CuNPs-containing composite film (Figure 10(d)) showed no signs of anthracnose. Inhibition activities based on the diameters of the anthracnose symptom demonstrated equal antifungal effects of the gelatin-starch coatings with and without CuNPs:

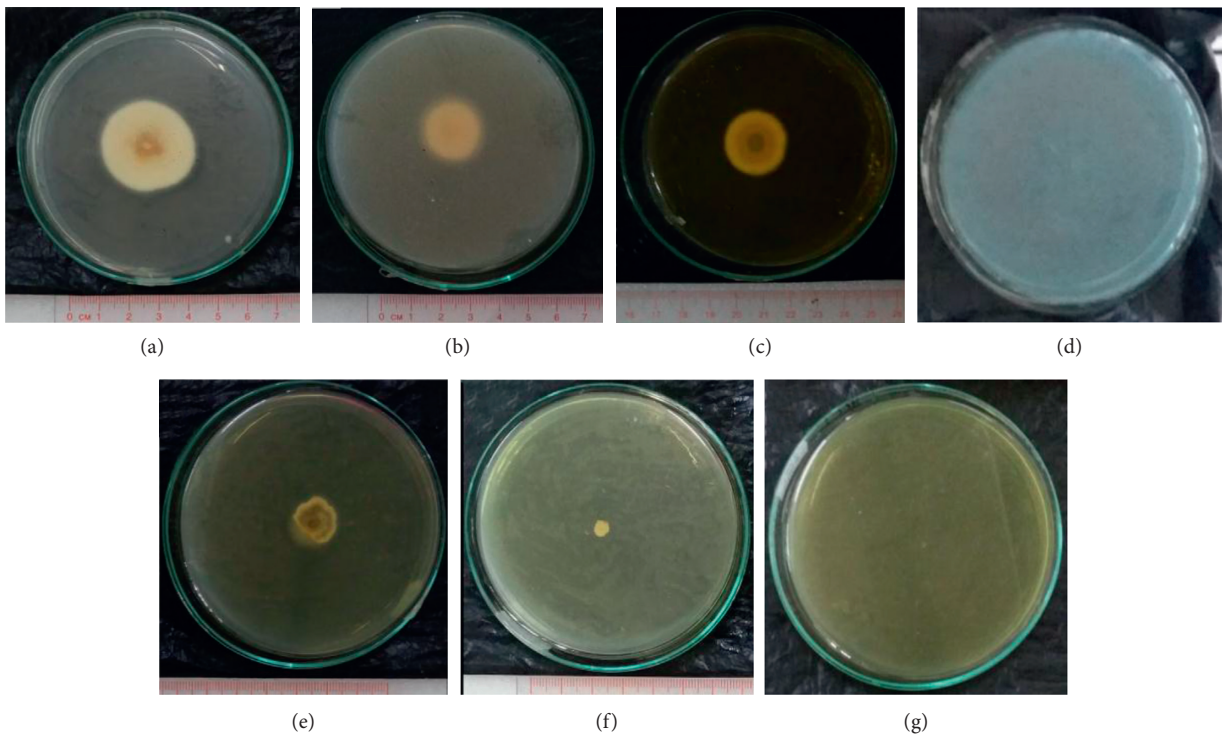

Figure 7: *C. gloeosporioides* colonies after 10 days of growth on nutrient agar containing (a) blank; (b) 20% mango flesh; (c) 2200 ppm AA; (d) 500 ppm $CuSO_4$; (e) 100 ppm CuNPs; (f) 150 ppm CuNPs; (g) 200 ppm CuNPs.

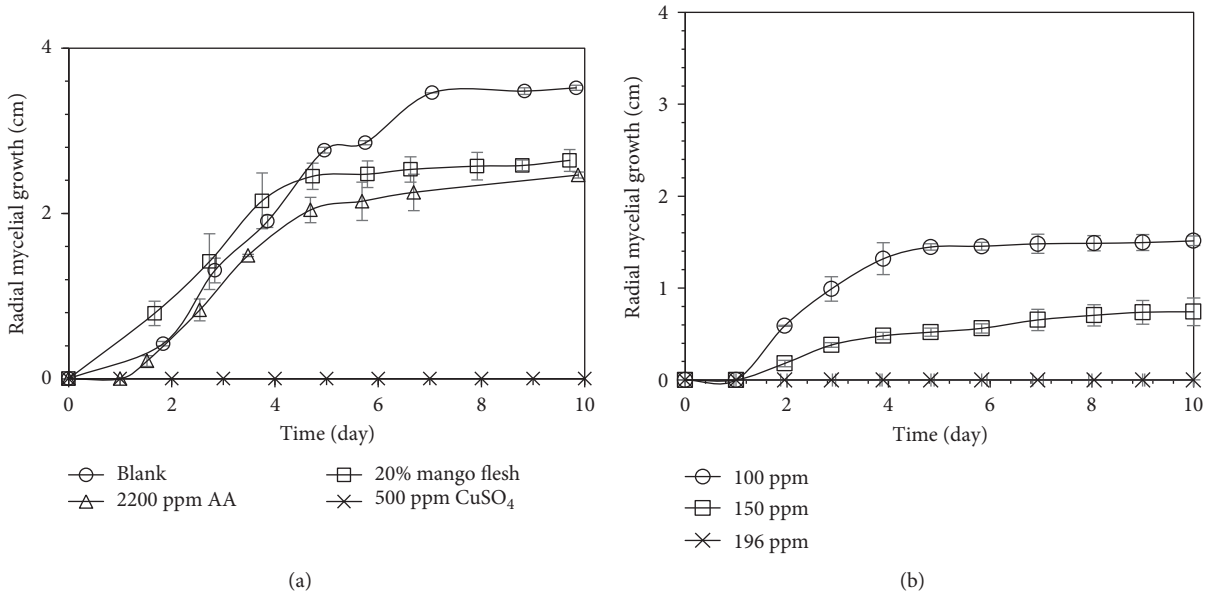

Figure 8: Growth dynamics of *C. gloeosporioides* on control media (a) and CuNPs-containing media (b).

84.44% and 84.77%, respectively. This result is contrary to that in the *in vitro* antifungal test for the films (Figure 9), where CuNPs-containing films exhibited higher antifungal activity. This contradictory result can be explained as follows.

Firstly, in the *in vivo* tests, the coatings completely covered the fruit surface and prevented the oxygen supply from the air to the fungus thanks to good gas-barrier properties of gelatin and starch [45,46]. In the *in vitro* tests, the films did not tightly cover the agar surface, thus ensuring the aerobic conditions for the fungal growth. Therefore, the fungus grew strongly with the control film without CuNPs. Secondly, the wet surface of agar promoted the growth of *C. gloeosporioides*, while the mango surface was much drier

(a) (b) (c)

Figure 9: *In vitro* antifungal test of the composite film containing 245 ppm CuNPs against *C. gloeosporioides* after 2 days. (a) Blank (without films). (b) Control (film without CuNPs). (c) Film with 245 ppm CuNPs.

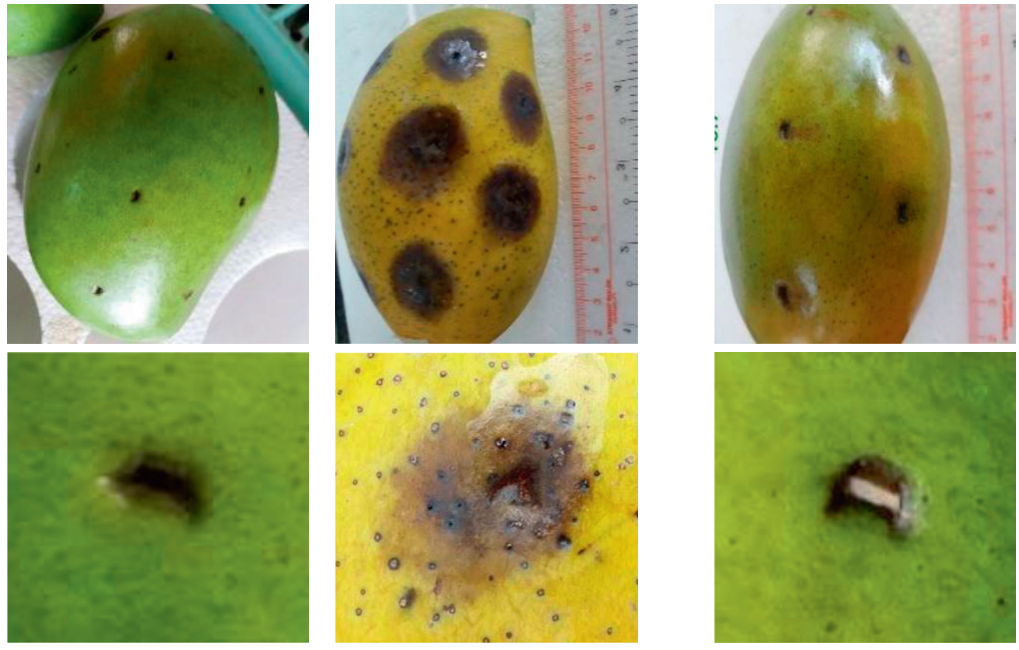

(a) (b) (c) (d)

Figure 10: *In vivo* antifungal test against *C. gloeosporioides* on the surface of mango: A1: 0^{th} day, CuNPs; B1: 4^{th} day, no coating; C1: 4^{th} day, control coating (without CuNPs); D1: 4^{th} day, coating with CuNPs. A2, B2, C2, D2 are magnified images of wounds in the A1, B1, C1, D1 figures, respectively.

and not suitable for the fungal growth [47]. This again implies that the antifungal activity of the CuNPs-containing film in the *in vitro* test was due to the diffusion of copper ions from the film to the agar surface.

4. Conclusions

CuNPs were synthesized using a green chemical approach, in which copper ions were reduced by AA in the presence of gelatin and glycerol as protecting agents. The identity and sizes of CuNPs were confirmed by XRD, TEM, and DLS results. CuNPs and tapioca starch-gelatin composite films containing CuNPs exhibited high *in vitro* antifungal activity against *C. gloeosporioides* causing anthracnose on mangoes. This *in vitro* activity is suggested to be due to the diffusion of copper ions from the surface of CuNPs into surroundings. *In vivo* assay on mango surface showed that the starch-gelatin coatings with and without CuNPs exhibit equally high antifungal activity against *C. gloeosporioides* due to the low oxygen permeability of the flour and gelatin coating. This study suggests that a non-toxic and edible film based on tapioca starch and gelatin can be used for protecting mangoes from anthracnose. Further studies with proper designs should be continued to separate the antifungal effects of the composite film and the CuNPs on mangoes, as well as to study the physiological and physicochemical

changes of the coated mangoes during storage, including copper contents in the peel and the flesh.

Data Availability

The data used to support the findings of this study are available from the corresponding author upon request.

Conflicts of Interest

The authors declare that there are no conflicts of interest regarding the publication of this paper.

Acknowledgments

The authors gratefully thank Ho Chi Minh City University of Technology and Education for facility and equipment support in completing this research.

References

[1] R. N. Tharanathan, H. M. Yashoda, and T. N. Prabha, "Mango (*Mangifera indica* L.), "the king of fruits"—an overview," *Food Reviews International*, vol. 22, no. 2, pp. 95–123, 2006.

[2] M. Kamle and P. Kumar, "*Colletotrichum gloeosporioides*: pathogen of anthracnose disease in mango (*Mangifera indica L.*)," in *Current Trends in Plant Disease Diagnostics and Management Practices*, pp. 207–219, Springer, Berlin, Germany, 2016.

[3] M. Schirra, S. D'Aquino, P. Cabras, and A. Angioni, "Control of postharvest diseases of fruit by heat and fungicides: efficacy, residue levels, and residue persistence: a review," *Journal of Agricultural and Food Chemistry*, vol. 59, no. 16, pp. 8531–8542, 2011.

[4] A. Kumar and V. Kudachikar, "Antifungal properties of essential oils against anthracnose disease: a critical appraisal," *Journal of Plant Diseases and Protection*, vol. 125, no. 2, pp. 133–144, 2018.

[5] L. F. Arauz, "Mango anthracnose: economic impact and current options for integrated management," *Plant Disease*, vol. 84, no. 6, pp. 600–611, 2000.

[6] D. Spalding and W. Reeder, "Decay and acceptability of mangos treated with combinations of hot water, imazalil, and gamma radiation," *Plant Disease*, vol. 70, no. 7, pp. 1149–1151, 1986.

[7] I. Koomen and P. Jeffries, "Effects of antagonistic microorganisms on the post-harvest development of Colletotrichum gloeosporioides on mango," *Plant Pathology*, vol. 42, no. 2, pp. 230–237, 1993.

[8] K. T. H. Dang, Z. Singh, and E. E. Swinny, "Edible coatings influence fruit ripening, quality, and aroma biosynthesis in mango fruit," *Journal of Agricultural and Food Chemistry*, vol. 56, no. 4, pp. 1361–1370, 2008.

[9] T. Huang, Y. Qian, J. Wei, and C. Zhou, "Polymeric antimicrobial food packaging and its applications," *Polymers*, vol. 11, no. 3, p. 560, 2019.

[10] S. A. Valencia-Chamorro, M. B. Pérez-Gago, M. A. Del Rîo, and L. Palou, "Curative and preventive activity of hydroxypropyl methylcellulose-lipid edible composite coatings containing antifungal food additives to control citrus postharvest green and blue molds," *Journal of Agricultural and Food Chemistry*, vol. 57, no. 7, pp. 2770–2777, 2009.

[11] S. A. Valencia-Chamorro, L. Palou, M. Á. del Río, and M. B. Pérez-Gago, "Performance of hydroxypropyl methylcellulose (HPMC)-lipid edible coatings with antifungal food additives during cold storage of "Clemenules" mandarins," *LWT—Food Science and Technology*, vol. 44, no. 10, pp. 2342–2348, 2011.

[12] E.-S. Park, H.-J. Lee, H. Y. Park, M.-N. Kim, K.-H. Chung, and J.-S. Yoon, "Antifungal effect of carbendazim supported on poly(ethylene-co-vinyl alcohol) and epoxy resin," *Journal of Applied Polymer Science*, vol. 80, no. 5, pp. 728–736, 2001.

[13] N. N. Van Long, C. Joly, and P. Dantigny, "Active packaging with antifungal activities," *International Journal of Food Microbiology*, vol. 220, pp. 73–90, 2016.

[14] P. Klangmuang and R. Sothornvit, "Active coating from hydroxypropyl methylcellulose-based nanocomposite incorporated with Thai essential oils on mango (cv. Namdokmai Sithong)," *Food Bioscience*, vol. 23, pp. 9–15, 2018.

[15] C. Maneerat and Y. Hayata, "Antifungal activity of TiO_2 photocatalysis against Penicillium expansum in vitro and in fruit tests," *International Journal of Food Microbiology*, vol. 107, no. 2, pp. 99–103, 2006.

[16] R. J. B. Pinto, A. Almeida, S. C. M. Fernandes et al., "Antifungal activity of transparent nanocomposite thin films of pullulan and silver against Aspergillus Niger," *Colloids and Surfaces B: Biointerfaces*, vol. 103, pp. 143–148, 2013.

[17] M. Rai, K. Kon, A. Ingle, N. Duran, S. Galdiero, and M. Galdiero, "Broad-spectrum bioactivities of silver nanoparticles: the emerging trends and future prospects," *Applied Microbiology and Biotechnology*, vol. 98, no. 5, pp. 1951–1961, 2014.

[18] M. A. Asghar, E. Zahir, S. M. Shahid et al., "Iron, copper and silver nanoparticles: green synthesis using green and black tea leaves extracts and evaluation of antibacterial, antifungal and aflatoxin B1 adsorption activity," *LWT*, vol. 90, pp. 98–107, 2018.

[19] A. P. Ingle, N. Duran, and M. Rai, "Bioactivity, mechanism of action, and cytotoxicity of copper-based nanoparticles: a review," *Applied Microbiology and Biotechnology*, vol. 98, no. 3, pp. 1001–1009, 2014.

[20] J. R. Lamichhane, E. Osdaghi, F. Behlau, J. Köhl, J. B. Jones, and J.-N. Aubertot, "Thirteen decades of antimicrobial copper compounds applied in agriculture. A review," *Agronomy for Sustainable Development*, vol. 38, no. 3, p. 28, 2018.

[21] S. Shende, N. Gaikwad, and S. Bansod, "Synthesis and evaluation of antimicrobial potential of copper nanoparticle against agriculturally important phytopathogens," *Synthesis*, vol. 1, no. 4, pp. 41–47, 2016.

[22] N. Pariona, A. I. Mtz-Enriquez, D. Sánchez-Rangel, G. Carrión, F. Paraguay-Delgado, and G. Rosas-Saito, "Green-synthesized copper nanoparticles as a potential antifungal against plant pathogens," *RSC Advances*, vol. 9, no. 33, pp. 18835–18843, 2019.

[23] B. Khodashenas and H. R. Ghorbani, "Synthesis of copper nanoparticles: an overview of the various methods," *Korean Journal of Chemical Engineering*, vol. 31, no. 7, pp. 1105–1109, 2014.

[24] D. Zhang and H. Yang, "Gelatin-stabilized copper nanoparticles: synthesis, morphology, and their surface-enhanced Raman scattering properties," *Physica B: Condensed Matter*, vol. 415, pp. 44–48, 2013.

[25] P. Chowdappa, G. Shivakumar, S. C. Chethana, and S. Madhura, "Antifungal activity of chitosan-silver nanoparticle composite against *Colletotrichum gloeosporioides*

associated with mango anthracnose," *African Journal of Microbiology Research*, vol. 8, no. 17, pp. 1803–1812, 2014.

[26] Q.-M. Liu, T. Yasunami, K. Kuruda, and M. Okido, "Preparation of Cu nanoparticles with ascorbic acid by aqueous solution reduction method," *Transactions of Nonferrous Metals Society of China*, vol. 22, no. 9, pp. 2198–2203, 2012.

[27] Y. A. Arfat, J. Ahmed, N. Hiremath, R. Auras, and A. Joseph, "Thermo-mechanical, rheological, structural and antimicrobial properties of bionanocomposite films based on fish skin gelatin and silver-copper nanoparticles," *Food Hydrocolloids*, vol. 62, pp. 191–202, 2017.

[28] J. Xiong, Y. Wang, Q. Xue, and X. Wu, "Synthesis of highly stable dispersions of nanosized copper particles using L-ascorbic acid," *Green Chemistry*, vol. 13, no. 4, pp. 900–904, 2011.

[29] A. Umer, S. Naveed, N. Ramzan, M. S. Rafique, and M. Imran, "A green method for the synthesis of copper nanoparticles using L-ascorbic acid," *Matéria (Rio de Janeiro)*, vol. 19, no. 3, pp. 197–203, 2014.

[30] N. L. Pacioni, V. Filippenko, N. Presseau, and J. C. Scaiano, "Oxidation of copper nanoparticles in water: mechanistic insights revealed by oxygen uptake and spectroscopic methods," *Dalton Transactions*, vol. 42, no. 16, pp. 5832–5838, 2013.

[31] J. Siegel, O. Kvítek, P. Ulbrich, Z. Kolská, P. Slepička, and V. Švorčík, "Progressive approach for metal nanoparticle synthesis," *Materials Letters*, vol. 89, pp. 47–50, 2012.

[32] B. K. Park, S. Jeong, D. Kim, J. Moon, S. Lim, and J. S. Kim, "Synthesis and size control of monodisperse copper nanoparticles by polyol method," *Journal of Colloid and Interface Science*, vol. 311, no. 2, pp. 417–424, 2007.

[33] D. Cho, D. Choi, R. C. Pawar et al., "Simple coating method of carbonaceous film onto copper nanopowder using PVP as solid carbon source," *Materials Chemistry and Physics*, vol. 148, no. 3, pp. 859–867, 2014.

[34] A. Ananth, S. Dharaneedharan, M.-S. Heo, and Y. S. Mok, "Copper oxide nanomaterials: synthesis, characterization and structure-specific antibacterial performance," *Chemical Engineering Journal*, vol. 262, pp. 179–188, 2015.

[35] X. Song, S. Sun, W. Zhang, and Z. Yin, "A method for the synthesis of spherical copper nanoparticles in the organic phase," *Journal of Colloid and Interface Science*, vol. 273, no. 2, pp. 463–469, 2004.

[36] B. Ankamwar, "Biosynthesis of gold nanoparticles (green-gold) using leaf extract of *Terminalia catappa*," *E-journal of Chemistry*, vol. 7, 2010.

[37] M. Stevanović, I. Bračko, M. Milenković et al., "Multifunctional PLGA particles containing poly(l-glutamic acid)-capped silver nanoparticles and ascorbic acid with simultaneous antioxidative and prolonged antimicrobial activity," *Acta Biomaterialia*, vol. 10, no. 1, pp. 151–162, 2014.

[38] V. Sreeja, K. N. Jayaprabha, and P. A. Joy, "Water-dispersible ascorbic-acid-coated magnetite nanoparticles for contrast enhancement in MRI," *Applied Nanoscience*, vol. 5, no. 4, pp. 435–441, 2015.

[39] M. Nor, N. Nazmi, and N. M. Sarbon, "Effects of plasticizer concentrations on functional properties of chicken skin gelatin films," *International Food Research Journal*, vol. 24, no. 5, 2017.

[40] H.-C. Kang, Y.-H. Park, and S.-J. Go, "Growth inhibition of a phytopathogenic fungus, *Colletotrichum* species by acetic acid," *Microbiological Research*, vol. 158, no. 4, pp. 321–326, 2003.

[41] B. Bagchi, S. Kar, S. K. Dey et al., "In situ synthesis and antibacterial activity of copper nanoparticle loaded natural montmorillonite clay based on contact inhibition and ion release," *Colloids and Surfaces B: Biointerfaces*, vol. 108, pp. 358–365, 2013.

[42] Y. Ohsumi, K. Kitamoto, and Y. Anraku, "Changes induced in the permeability barrier of the yeast plasma membrane by cupric ion," *Journal of Bacteriology*, vol. 170, no. 6, pp. 2676–2682, 1988.

[43] Y. Wei, S. Chen, B. Kowalczyk, S. Huda, T. P. Gray, and B. A. Grzybowski, "Synthesis of stable, low-dispersity copper nanoparticles and nanorods and their antifungal and catalytic properties," *The Journal of Physical Chemistry C*, vol. 114, no. 37, pp. 15612–15616, 2010.

[44] G. D. L. Po, M. Sanvictores, M. C. L. Baticados, and C. R. Lavilla, "*In vitro* effect of fungicides on hyphal growth and sporogenesis of *Lagenidium spp.* isolated from *Penaeus monodon* larvae and *Scylla serrata* eggs," *Journal of Fish Diseases*, vol. 5, no. 2, pp. 97–112, 1982.

[45] R. Sothornvit and N. Pitak, "Oxygen permeability and mechanical properties of banana films," *Food Research International*, vol. 40, no. 3, pp. 365–370, 2007.

[46] S. F. Hosseini, Z. Javidi, and M. Rezaei, "Efficient gas barrier properties of multi-layer films based on poly(lactic acid) and fish gelatin," *International Journal of Biological Macromolecules*, vol. 92, pp. 1205–1214, 2016.

[47] A. B. Estrada, J. C. Dodd, and P. Jeffries, "Effect of humidity and temperature on conidial germination and appressorium development of two Philippine isolates of the mango anthracnose pathogen *Colletotrichum gloeosporioides*," *Plant Pathology*, vol. 49, no. 5, pp. 608–618, 2000.